The Perfect Fluid Characteristic of the Quark Gluon Plasma

Ke Li[1], Cheng Ma[2, *], Jiahua Qu[3], Jiayi Zhang[4]

[1]Experimental Middle School Affiliated to Beijing Normal University, Beijing, 100032, China, Jim_Leek@hotmail.com.
[2]College of Mechanical Engineering, Tianjin University, Tianjin, 300254, China, 3020001568@tju.edu.cn.
[3]Beijing 80th Middle School Wangjing Campus, Beijing, 100102, China, michaelquu070308@icloud.com.
[4]Winchester Thurston School, Pittsburgh, PA, 15213, USA, ZhangJ@winchesterthurston.org.
*Corresponding author email: 3020001568@tju.edu.cn

Abstracts: This article explores the unique characteristics of the Quark Gluon Plasma (QGP) by analyzing open data obtained from the ALICE experiment for Pb-Pb collisions and from the CMS experiment for Xe-Xe collisions at the Large Hadron Collider (LHC). The total integrated luminosity of the analyzed data is 3.42 μb^{-1}. The findings indicate that there are similar patterns in the correlation between the transverse momentum (P_t) and the flow coefficients (v_2 and v_3) in both Xe-Xe and Pb-Pb collisions. Additionally, the paper estimates the shear viscosity to entropy density ratios of the QGPs by comparing the P_t dependence of v_2 and v_3, as obtained from the experiments, with the calculations derived from relativistic hydrodynamics equations using various shear viscosity to entropy density ratios.

Keywords: QGP, perfect liquid, shape fluctuations, anisotropic flow, shear viscosity

1. Introduction

1.1 QGP

About 15 billion years ago, the Big Bang occurred. The Big Bang created an environment of extremely high temperature and density, which produced a large number of quarks, antiquarks and gluons that interacted strongly to form the quark-gluon plasma, after which the Universe expanded and cooled down to form the material world we now live in.

Free quarks have never been observed, and the theory suggests that quarks and gluons are confined within the hadron by strong interactions. At the same time, the theory predicts that hadrons will be produced out of confinement at extremely high temperatures and high baryon densities, and the QCD phase diagram (Fig.1)

graphically demonstrates that phase transitions of nuclear matter can occur at the extremes of high temperatures and high baryon densities [1].

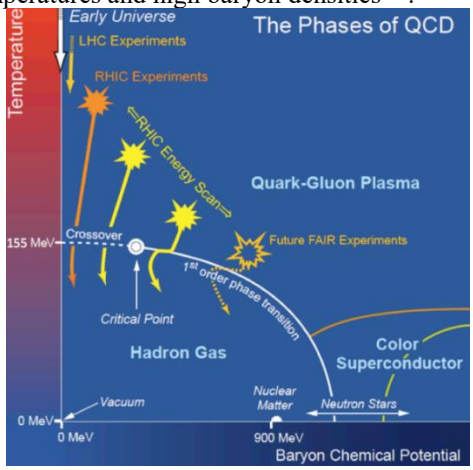

Fig1. The Phases of QCD [1]

Experimental methods involving relativistic heavy-ion collisions are employed for the purpose of generating quark-gluon plasmas (QGPs). This involves accelerating two nuclei close to the speed of light and subsequently causing them to collide. The subsequent collision results in high temperatures and pressures, leading to the deconfinement of the nuclei and the formation of a quark-gluon plasma. A visual representation of this process is depicted in Figure 2, showcasing a cross-section of a relativistic heavy ion pre- and post-collision [2].

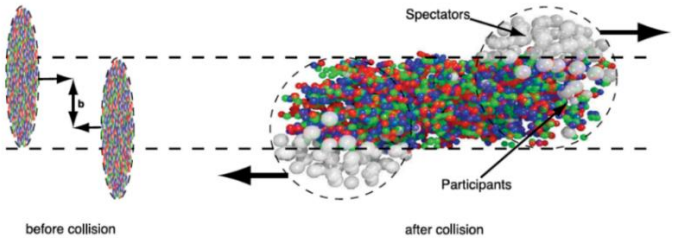

Fig2. Schematic cross section before and after relativistic heavy ion collisions [2]

Figure 3 illustrates the schematic representation of the evolution of relativistic heavy ion collisions [3]. During the collision of high-speed "discs", the energy density in the collision region rapidly increases, leading to the decoupling of nuclei and the generation of a significant number of quarks, antiquarks, and gluons. The intense interactions between these elementary particles drive the system towards thermal equilibrium, resulting in the formation of a quark-gluon plasma. As the collision system expands and cools down, some of the hadrons undergo hadronization,

followed by their subsequent scattering. Eventually, the hadrons escape the reaction system and are detected.

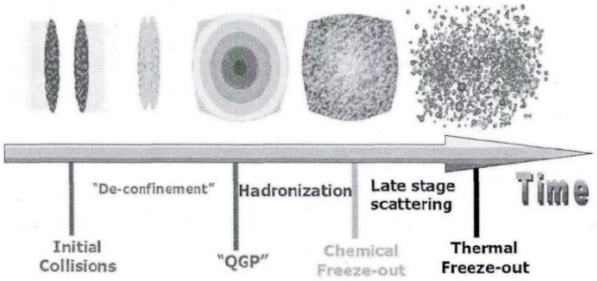

Fig3. a schematic of the evolution of relativistic heavy-ion collisions [3]

For the past experiments, RHIC (relativistic heavy ion collider) and LHC (large hadron collider) separately imposed $\sqrt{S_{NN}} = 200GeV$ to $Au + Au$ collision and $\sqrt{S_{NN}} = 5.02\,TeV$ to $Pb + Pb$ collision. Those collisions have revealed horrendous characteristics of the QGP. For example, the most ideal fluid, high vorticity and strong magnetic field.

1.2 Anisotropic Flow

Anisotropic flow is a result of the initial geometry of the hot dense matter produced by heavy ion collisions and is therefore sensitive to the early properties of the evolution of the hot dense matter. The quantification of this property can be achieved through the Fourier expansion of the azimuthal distribution of particles with respect to the reaction plane.

where ϕ is the azimuth of the particle and Ψn is the azimuth of the reaction plane in the laboratory system. The first three coefficients of the Fourier expansion are the direct flows, elliptic flows, and triangle flows, i.e., $v1$ denotes the strength of the direct flows, $v2$ denotes the strength of the elliptic flows, and $v3$ denotes the strength of the triangle flows. $v3$ denotes the strength of triangle flows. In fact, the anisotropic flow originates from the transformation of the anisotropy of the initial space to the anisotropy of each of the azimuthal angles in the momentum space, as shown in Fig. 4[4]

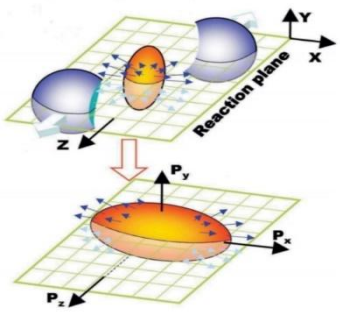

Fig.4. Schematic diagram of elliptical flow produced by relativistic heavy ion non-central collisions [4]

2. Calculation of v_2 and v_3

In the measurement of elliptic flows using azimuthal correlations, some of the correlations come from correlations other than the initial geometry, such as decays of resonance states, jets, fragmentation of hard scattering partons, and so on. The strength of the non-flows is considered to be related to the multiplicity of charged particles N_{ch} with $1/N_{\mathrm{ch}}$ in the two-particle measurement process [5], while in the four-particle measurement process, the contribution from the non-flow is related to the charged particle multiplicity by $1/N_{\mathrm{ch}}^3$ [5].

Therefore, in large-system collisions (e.g., $Au-Au$, $Pb-Pb$), the noncurrent contribution is greatly compressed due to the larger particle multiplicity Nch produced by the collision. In contrast, during small-system collisions (e.g., proton-proton, proton-lead), a relatively large contribution to nonflow is produced due to the smaller number of particles produced by the collisions and thus the relatively large contribution to nonflow. In two-particle correlation measurements of the collective flow, the noncurrent component has an impact on the collective flow size, since the collective flow size is given by the Fourier series expansion of the azimuthal equation. Therefore, two-particle correlations with a large rapidity interval ($\Delta\eta$) are usually only considered for the purpose of compressing the non-flow.

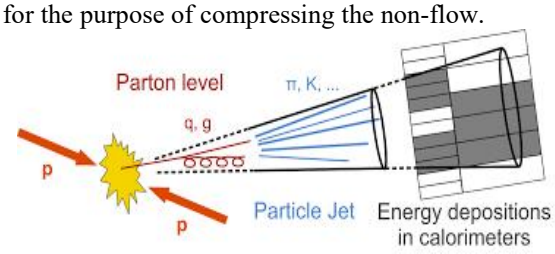

Fig 5. Production of particle jets

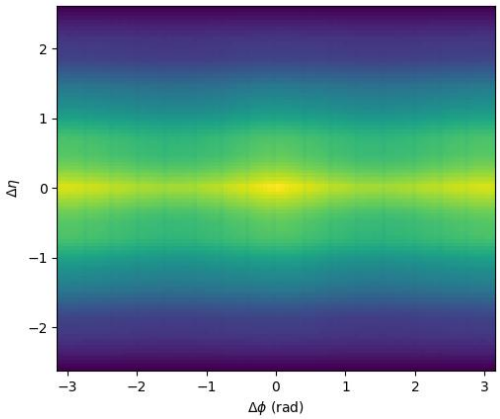

Fig 6. Correlation between $\Delta\varphi(-\pi\sim\pi)$ and $\Delta\eta(-1\sim1)$

The final emitted particles can be expressed within two coordinates: the configuration coordinate (x, y, z), and the momentum coordinate (P_t, η, Φ).

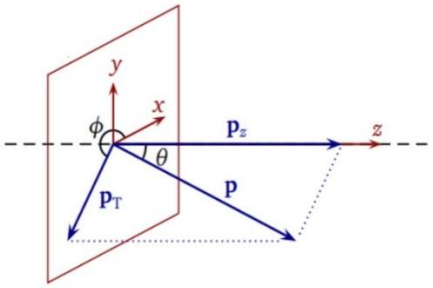

Fig 7. coordinate showing the final momentum of the emitted particle.

In order to find the momentum along each direction within the configuration coordinate, we can adopt some simple calculations with measure data. With the transverse momentum P_t, and the angle Φ, we can calculate the x and y components of the total momentum as (3) and (4) shows:

$$P_x = P_t \times cos\,\Phi \text{ .....（1）}$$

$$P_y = P_t \times sin\,\Phi \text{ .....（2）}$$

With the measured data, η, we can find θ:

$$\eta = -\ln tan\left(\frac{\theta}{2}\right) \text{ .....（3）}$$

$$P_z = P \times cos\,\theta \text{ .....（4）}$$

$$P = \sqrt{P_x^2 + P_y^2 + P_z^2} \text{.....（5）}$$

Knowing Px, Py and θ, we can solve this equation set to find the z component of the total momentum.

The Fourier expansion of the azimuthal correlation function is [6]:

$$\frac{\mathrm{d}N}{\mathrm{d}\Delta\phi} = N[1 + 2v_2^2 \cos(2\Delta\phi) + 2v_3^2 \cos(3\Delta\phi)] \text{.....(6)}$$

The $dN/d\Delta\phi$ from the open data of ALICE Pb-Pb collision experiment at LHC and the fitted correlation between $dN/d\Delta\phi$ and $\Delta\phi$ using Eq (9) are shown in Fig.11. While taking the first two terms of the Fourier decomposition of the azimuthal distribution function for fitting to obtain Fig.11(a), where $v_2 = 1.48211340e-01$; while taking the first three terms for fitting to obtain Fig.13, where $v_3 = 1.48275351e-01$, $v_3 = -5.31178879e-02$. It could be observed that the curve generated using v_2 and v_3 fits the experimental data better than the curve generated using the term v_2 solely. The gaps in the figure are probably caused by the detector's inability to detect particles moving in certain azimuthal angles.

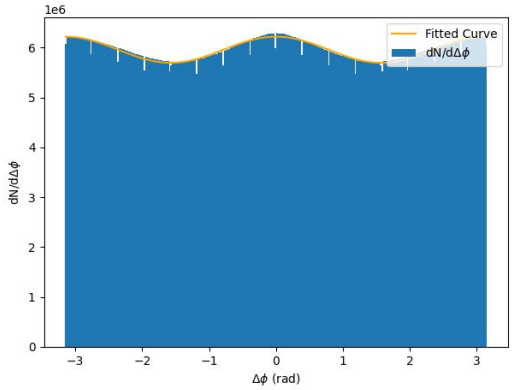

(a)

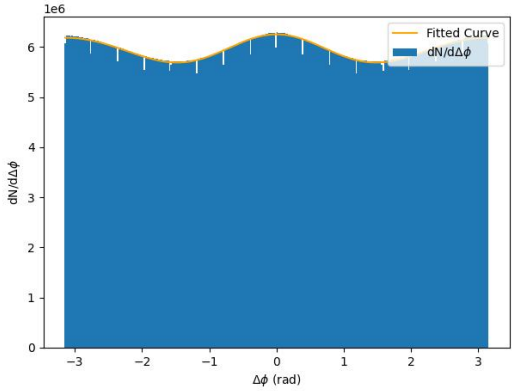

(b)

Fig 8. Histograms and Fitted Curves of the Azimuthal Correlation Function

The Fourier coefficients v_2 and v_3 :

$$v_2 = \langle cos\left(2(\phi - \psi_2)\right)\rangle \text{.....（7）}$$

$$v_3 = \langle cos\left(3(\phi - \psi_3)\right)\rangle \text{.....（8）}$$

In (9) and (10), ψ_2 and ψ_3 represents the minor axis of the elliptic flow and the minor axis of the triangular flow that are shown in Fig.3.

$$\psi_2 = \frac{arctan\,2(\langle r^2 \sin(2\phi^{part})\rangle, \langle r^2 cos(2\phi^{part})\rangle) + \pi}{2} \text{.....(9)}$$

$$\psi_3 = \frac{arctan\,2(\langle r^2 \sin(3\phi^{part})\rangle, \langle r^2 cos(3\phi^{part})\rangle) + \pi}{3} \text{.....(10)}$$

By plugging (12) and (13) into (10) and (11), we can easily approach the values of the elliptic flow and triangular flow, which act as the final conditions of our calculation.

3. The Perfect Fluid and Viscosity

Since the density of QGP is around ten to the twenty times larger than water which makes it hard to compare the viscosity of QGP with other daily fluid, the shear viscosity to entropy density ratio (η/s) is introduced. Placing the entropy density at the denominator effectively wipes out the overwhelming density of QGP when comparing the viscous effect. Considering the modern physics perspective, the Kubo formulae can obtain the shear viscosity by analyzing the linear response and fluid-gravity coupling [7]:

$$\eta = \lim_{\omega \to 0}\left(\frac{1}{2\omega}\int dt d\bar{x} e^{i\omega t}\langle[T_{xy}(t,\bar{x}), T_{xy}(0,\bar{0})]\rangle\right) \text{.....（11）}$$

This equation can be used to calculate h/s under the circumstance of the AdS/CFT correspondence. In order to do that one starts from a CFT with gravity dual. The dual theory is a CFT (conformal field theory) at temperature T equal to the Hawking temperature of the black-brane and entropy $S = A/4G_N$. As the graviton is polarized within x-y plane, the imaginary part in Green's function is coupled with the metric. Then we can get [8]:

$$\eta = \frac{\sigma(0)}{16\pi G_N} \text{.....（12）}$$

where $s(0)$ is the graviton absorption cross-section at zero energy.

As the result η/s ratio with gravity dual is yielded, the Kovtun, Son and Starinets (KSS) proposed that for a broad range of systems, including those that can only be explained by the quantum field theory, the lower bound of the η/s is $1/4\pi$ [9]. The experiments that RHIC conducted may have created a significant amount of the collective flow before the plasma area rebound themselves into hadrons. The lowest η/s ratio of the collective flow in the QGP area is around 0.08 which is the least value ever presented.

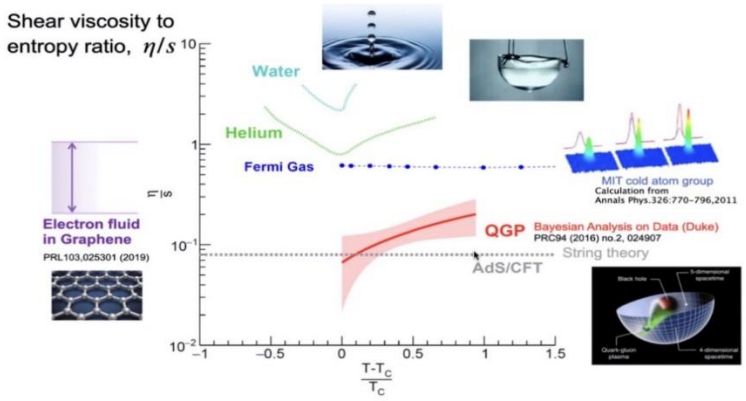

Fig 9. η/s value under different temperature, including water, helium and QGP.

With the value of the ε_2 and ε_3, v_2 and v_3, we can put the η/s value and determine if the ratio fits in the situation. The shear viscosity causes the anisotropic deviation from the equilibrium. Its main effect is that it reduces the gap of the expansion along each direction when the QGP is formed by using the shear viscous tensor $\boldsymbol{\pi^{ij}}$ to reduce the longitudinal pressure and promotes the transverse pressure.

Using different $\frac{\eta_s}{S}$, we will obtain different correlation between p_t, v_2, v_3. We will determine $\frac{\eta_s}{S}$ by finding out which value of $\frac{\eta_s}{S}$ gives the p_t, v_2, v_3 dependence that best fits with our experiments. Fig 13 (a) shows the correlation between P_t and v_2 and v_3 and Fig.13 (b) shows the correlation between P_t and v_2 for different $\frac{\eta_s}{s}$ obtained by solving relativistic hydrodynamic equations (adapted from Sirunyan A M, Tumasyan A, Adam W, et al [10]).

The P_t dependence of v_2 and v_3 for Pb-Pb collision and Xe-Xe collision with centrality between 40% - 50% is compared in Fig.13 (a). It could be observed that the P_t dependence of v_2 and v_3 follows similar patterns.

The range of low transverse momentum ($P_t < 3GeV$), the elliptic flow parameter v_2 and the delta flow parameter v_3 for $Xe-Xe$ and $Pb-Pb$ collisions both show a monotonically increasing trend with P_t, whereas, after the value of Pt exceeds $3GeV$, v_2 and v_3 for both $Pb-Pb$ and $Xe-Xe$ start to decrease with the increase of the value of Pt and the value of v_2 is larger than v_3 for both $Pb-Pb$ and $Xe-Xe$ are greater than v_3. And for different collisional centripetal and transverse momentum conditions, the values of the elliptic flow parameter v_2 decrease as the value of the approximated viscosity coefficient η/s increases.

It is also observed that the η/s ratio of Pb-Pb and Xe-Xe collisions is approximately 0.08.

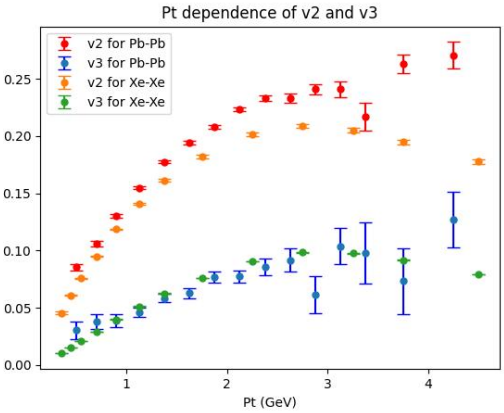

(a)

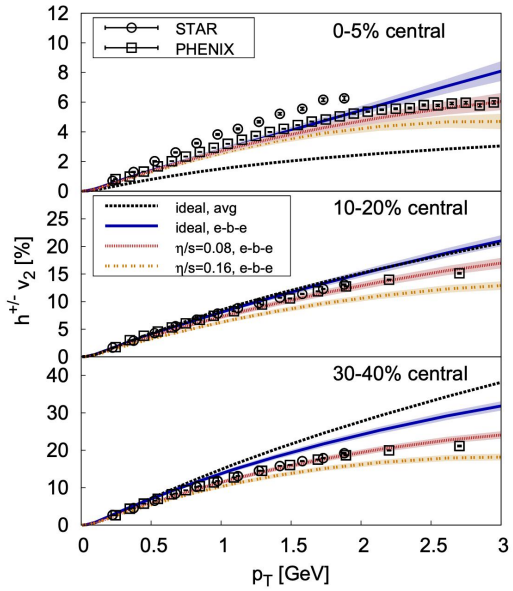

(b)

Fig.10 (a) P_t dependence v_2 and v_3 (b) Correlation between P_t and v_2 for different $\frac{\eta_s}{s}$ (adapted from Sirunyan A M, Tumasyan A, Adam W, et al[10])

4. Conclusion

This paper presents a discussion on the characteristics of anisotropic flow and low viscosity observed in the quark gluon plasma (QGP), which behaves as a perfect fluid. The anisotropic flow of the QGP originates from the conversion of the initial anisotropy in shape-space within the interaction region to the anisotropies in the

momentum space of the final-state particles after a nucleus-nucleus collision. These anisotropic flows can be categorized as direct, elliptic, and triangular flows, with their magnitudes determined by the coefficients of the first three orders obtained through Fourier decomposition of the azimuthal distribution function of the final-state particles.

The state information of the end-state particles is described using the transverse momentum (P_t), azimuthal angle (Φ), and pseudo-rapidity (η) within a laboratory coordinate system. By using these variables, we can compute the elliptic flow parameter (v_2) and the triangular flow parameter (v_3).

The results by analyzing public data from the ALICE experiment for Pb-Pb collisions and the CMS experiment for Xe-Xe collisions at the Large Hadron LHC reveal consistent trends in the relationship between transverse momentum (P_t) and flow coefficients (v_2 and v_3) for both Xe-Xe and Pb-Pb collisions. It is estimated that the QGP's shear viscosity to entropy density ratios is approximately 0.08 by comparing the experimentally observed Pt dependence of v_2 and v_3 with the computed values derived from relativistic hydrodynamics equations utilizing η/s.

References

[1] Akiba Y, et al. The Hot QCD White Paper: Exploring the Phases of QCD at RHIC and the LHC [J]. 2015.

[2] Ploskon M. Heavy-ion collisions - hot QCD in a lab [J]. arXiv e-prints, 2018: arXiv:1808.01411.

[3] Xiao K. Study of anisotropic flow in relativistic heavy ion collisions and its rise and fall and event plane correlation [D]. Central China Normal University,2014.

[4] Heinz U W. The Strongly coupled quark-gluon plasma created at RHIC [J/OL]. J. Phys. A, 2009, 42: 214003.

[5] Borghini N, Dinh P M, Ollitrault J Y. Flow analysis from multiparticle azimuthal correlations [J/OL]. Phys. Rev. C, 2001, 64: 054901.

[6] J. Bleibel, G. Burau, C. Fuchs, Anisotropic flow in Pb + Pb collisions at LHC from the quark–gluon string model with parton rearrangement [J]. Phys. Lett. B. 659,537 (2008)

[7] B.Alver, G.Roland. Collision geometry fluctuations and triangular flow in heavy-ion collisions [J]. Phys.Rev.C,81:054905,2010

[8] MA Y, ZHOU C, FANG D. Ratio of viscosity coefficient to entropy density in the participant region in medium-energy heavy-ion collisions[J]. Nucl. Phys. Rev,2014,31(03):315-325.

[9] Sirunyan A M, Tumasyan A, Adam W, et al. Charged-particle angular correlations in XeXe collisions at s N N= 5.44 TeV[J]. Physical Review C, 2019, 100(4): 044902.

[10] Schenke B, Jeon S, Gale C. Elliptic and triangular flow in event-by-event D= 3+ 1 viscous hydrodynamics[J]. Physical review letters, 2011, 106(4): 042301.